ADVANCED INTELLIGENT SYSTEMS Open Access
www.advintellsyst.com

Wind Defiant Morphing Drones

Charalampos Vourtsis, Victor Casas Rochel, Nathan Samuel Müller, William Stewart, and Dario Floreano*

Intense winds are a challenge for vertical take-off and landing drones with wings. In particular, in the hovering regime, wings are sensitive to wind currents that can be detrimental to their operational and energetic performances. Tail-sitters are particularly prone to those wind currents because their wings are perpendicular to the incoming wind during hovering. This wind generates a large amount of drag and can displace and destabilize the vehicle, possibly leading to catastrophic failures. Herein, our morphing strategy demonstrates in a custom-built 1.8 kg tail-sitter with morphing wings that can actively resist winds and leverage them to increase its aerodynamic efficiency. It is shown that adaptive wing morphing during hovering in adverse wind conditions can reduce normalized energy consumption up to 85%, increase attitude and positional stability, and leverage wind energy to increase its yaw angular rate up to 200% while decreasing motor saturation levels.

1. Introduction

Hybrid unmanned aerial vehicles (UAVs) refer to drones that combine the benefits of fixed-wing and rotary-wing aircraft in that they are capable of both horizontal and vertical (hovering) flight operations.[1] Most hybrid UAVs reorient the entire propulsion system or use a dedicated propulsion unit for each flight mode.[1,2] The reorientation of the propulsion system, or the presence of additional propulsion units, increases the mechanical complexity and weight of these UAVs, resulting in reduced energy efficiency. Tail-sitters are a type of hybrid UAV with fixed wings capable of hovering and transitioning to horizontal flight without reorienting the propulsion system or dedicated propulsion units. The tail-sitter design has the lowest mechanical complexity, but the exposed wings leave the vehicle particularly prone to crosswinds in hovering flight.[2]

C. Vourtsis, V. C. Rochel, N. S. Müller, W. Stewart, D. Floreano
Laboratory of Intelligent Systems
Ecole Polytechnique Federale de Lausanne
Lausanne CH1015, Switzerland
E-mail: harry.vourtsis@epfl.ch

The ORCID identification number(s) for the author(s) of this article can be found under https://doi.org/10.1002/aisy.202200297.

DOI: 10.1002/aisy.202200297

In nature, flying animals, like birds and insects, operate in diverse wind conditions by adapting their wing morphology or body configuration according to the flight performance they need to achieve.[3] Birds change the shape of their wings to increase or decrease their agility, and insects rapidly change their flapping angles to perform highly agile maneuvers.[4–6] Wing morphing is a commonly adopted strategy by engineers, although current vehicles fail to achieve the performance of natural flyers.[7] Nevertheless, different approaches have already been proposed as solutions for gust rejection and increased maneuverability in the hovering regime of vertical take-off and landing (VTOL) platforms. Sweeping wings are retracted during hovering to reduce the moment of inertia, thus increasing maneuverability.[8,9] However, in the work of Ang et al., the area of the wings remains unchanged throughout the flight, and therefore, the vehicle's performance in crosswinds does not change.[8] In contrast, in the work of Heredia et al., the wings are entirely retracted in hovering, thus not providing any possible aerodynamic benefit as it would be in the cases where the drone is flying with the wind.[9] Another solution for wind rejection is to adapt the wing design to enforce flow detachment in the airfoil's leading edge to mitigate turbulent perturbations. However, this solution would not be applicable in wings oriented perpendicular to crosswinds where the wings are in deep stall, and the drag effects are predominant to the lift generation.[10] Furthermore, biologically inspired morphing wings attract interest to make winged drones more agile in wind conditions, but these do not specifically address the problem of withstanding adverse winds or hovering flight.[10–12] Other topics of work that focus explicitly on mitigating wind effects concentrate on controller development, although they do not address wind energy harvesting.[13–15] Rather than simply reducing the adverse wind effects, other studies show the possibility of harvesting energy to increase range and endurance by exploiting thermal wind currents. This approach is widely investigated for powered and unpowered fixed-wing soaring.[16–19] However, this particular strategy requires the aircraft to continuously pass through air masses with different speeds and at specific angles of attack, which is not the primary mode of operation profile of VTOL platform in hovering, where it is required to fly for long periods at angles of attack of more than 60°.

In this work, we describe a strategy where we utilize the morphing wings of a VTOL platform in such a way that we increase stability against adverse winds while leveraging

wind energy for efficient hovering flight and increased maneuverability in the yaw axis (**Figure 1**A).

The wing area has a strong impact on flight performance. A large wing area increases the vulnerability to cross winds during hovering operations due to large amounts of generated drag. Therefore, VTOLs with fixed wings usually face a design compromise. There is a trade-off between small wing size for smaller drag during hovering flight and larger wing size for increased lift during horizontal flight.

We overcome this compromise by either symmetrically or asymmetrically changing the drone's wing area based on the wind direction. This is accomplished with a wing controller that can adjust the wing area of the drone using simple servo actuators. The principle is based on minimizing the overall energy consumption and not solely on drag reduction or lift maximization. This means that the controller can exploit crosswinds in a beneficial manner depending on if the next commanded waypoint is upwind or downwind of the vehicle. Similarly, we utilize asymmetric morphing to exploit wind currents for yaw control or to increase the drone's maximum achievable yaw rate when used in conjunction with motor actuation. By commanding wing asymmetry in windy conditions, yaw control can be decoupled from maintaining altitude or assisted by the wing morphing. Controlling yaw only through deferentially actuated motors exhibits a yaw rate threshold that occurs due to the motors needing to maintain altitude and turn the vehicle simultaneously.

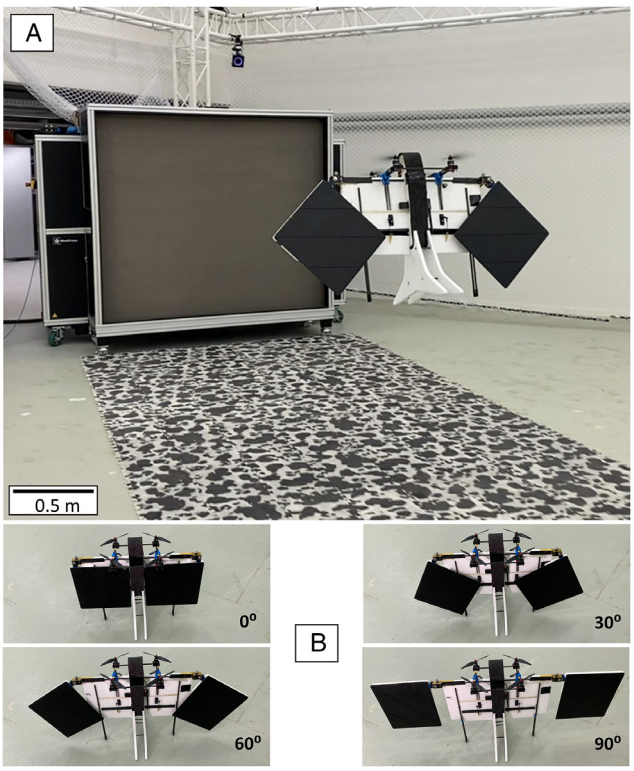

Figure 1. A) A morphing vertical take-off and landing (VTOL) tail-sitter drone in front of the windshape wind generator.[22] B) Symmetric wing configurations of the morphing VTOL tail-sitter.

2. Morpho—A Morphing Vertical Take-Off and Landing Drone

Morpho is a quad tail-sitter UAV with morphing wings that adapt their surface depending on the flight mode and wind conditions (Figure 1). The drone's extended and retracted configurations along with the effects of wing morphing in the center of gravity and the moments of inertia are presented in **Figure 2**. For simplicity, the wing has a rectangular airfoil profile with a thickness of ≈15 mm.

The drone is utterly autonomous during flight (**Figure 3**). For the autonomous flight experiments, a Pixhawk 4 autopilot is utilized in conjunction with a Jetson Nano companion computer on a carrier board modified for weight reduction. The companion computer is required to run the wing controller parallel to the autopilots' function. The companion computer receives information from the autopilot through MAVROS, an robot operating system (ROS) bridge for the MAVLink protocol. It uses the state estimation and the trajectory setpoints from the autopilot to adaptively morph the wings. It does so by sending commands to the servo actuators through Dynamixel protocol 2.0 (Figure 3). All the hardware components are connected serially. The wing servo controller's functionality is generalized and independent from the autopilot as it uses the calculated yaw rate error as input. Therefore, different autopilots could provide the yaw rate setpoint and state estimation.

While wind estimation in actual missions can be estimated either by a wind sensor or changes in the state estimate, the current prototype does not utilize a wind estimation method for simplification.

3. Aerodynamic Characterization

Experiments were performed to investigate the aerodynamic properties of the different wing morphing configurations. A 6 degrees of freedom (DOF) ATI Gamma loadcell was mounted to the bottom part of the drone at its center of gravity (**Figure 4**). Through combinations of different wing morphing states, eight configurations were characterized. These correspond to both symmetric and asymmetric wing morphing configurations for wing sweep angles of 0°–90° with increments of 30°. Similar to,[20,21] the drone was attached to a Stäubli robotic arm that was placed in an open-jet WindShape wind tunnel.[22] The robot was programmed to drive the robot through a commanded angle of attack. The angle of attack, defined as zero when the vehicle is hovering vertically, was varied between 40° and −50° starting from 0° and in increments of 4°. The drone was positioned such that the fuselage of the drone is approximately 50 cm from the wind tunnel filter. Experiments were run at wind speeds of 1.7, 3.4, and 4.6 m s^{-1} measured at the beginning of the free stream, which corresponds to Reynolds numbers of 35 898, 71 796, 97 135 as calculated with the reference length of the morphing wing when horizontal to the flow. Data samples were recorded at 120 Hz after the wing flow had reached a steady state. Recorded forces were rotated to the wind frame to calculate lift, drag, and yawing moments.

The aerodynamic results, which are displayed in **Figure 5**, show an increase in lift and a decrease in drag as the plane shifts from the 0° position (A), (B), (D). Drag increases significantly in

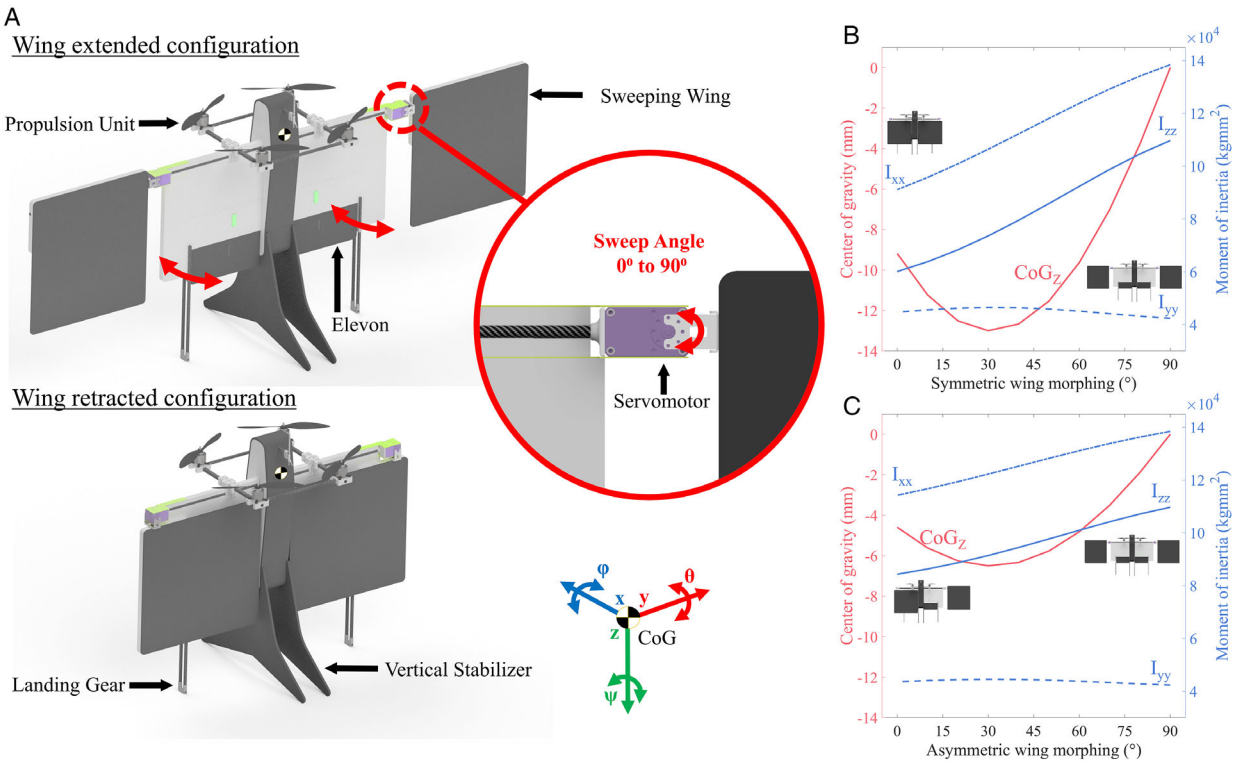

Figure 2. A) A morphing VTOL tail-sitter drone, in its extended and retracted wing configurations, with detail in its sweeping wing servo mechanism. The drone's weight is 1.8 kg. The drone with wings unfolded has a wingspan of 1.45 m and a wing area of 0.44 m^2, while with the wings retracted, it has a wingspan of 0.79 m and a wing area of 0.29 m^2. The length of the fuselage is 0.62 m. The propulsion system consists in four propellers in tractor mode actuated by four Rctimer 28 301 000 KV brushless motors with a 45 A four-in-one electronic speed controller (ESC). For the wing actuation, two Dynamixel XM430-W350-T servomotors are used. Elevons are only used for attitude control in forward flight. A lithium polymer battery of 2500 mAh in a four-cell configuration powers the drone. The fuselage and the wings are made from cardboard and expanded poly propylene (EPP), a foam material with high mechanical resilience and flexibility. The center of gravity is depicted in both configurations. Carbon beams were used to reinforce the structure and to mount the two servo actuators (Dynamixel XM430-W350-T) used to fold the wing tips. The motor mounts, the servo actuator mounts, and landing gear components were 3D printed with acrylonitrile butadiene styrene (ABS) plastic. B) Change in the center of gravity (CoG) in the *z*-axis and moments of inertia (I*xx*, I*yy*, I*zz*) in symmetric wing morphing. C) Change in the center of gravity (CoG) in the z-axis and moments of inertia (I*xx*, I*yy*, I*zz*) in asymmetric wing morphing.

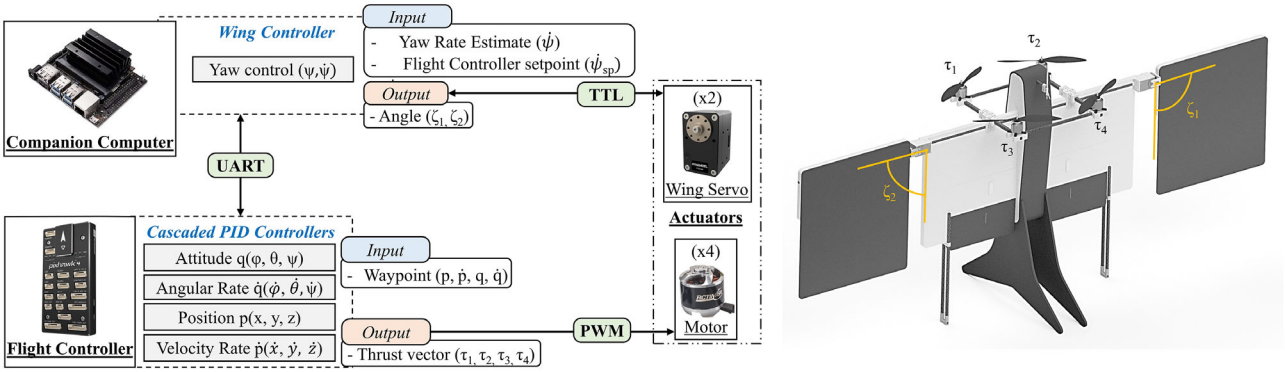

Figure 3. High-level controller architecture. A P controller is deployed for controlling the wing morphing state when the wings are used for actively stabilizing yaw. It takes as input the yaw rate error computed by the flight controller[25] and outputs the desired wing angle magnitude (ang_magn). According to the wind direction (wind_dir_sign) in the body frame, the commanded wings angle is [–wind_dir_sign ang_magn, wind_dir_sign ang_magn]. This command is then clipped between [0,pi/2] and sent to the servomotors, which track a trapezoidal velocity profile with an acceleration of 18.73 rad s^{-2} and a top speed of 2.4 rad s^{-1}. The companion computer communicates with the autopilot through MAVROS, which is a ROS bridge for the MAVLink protocol.

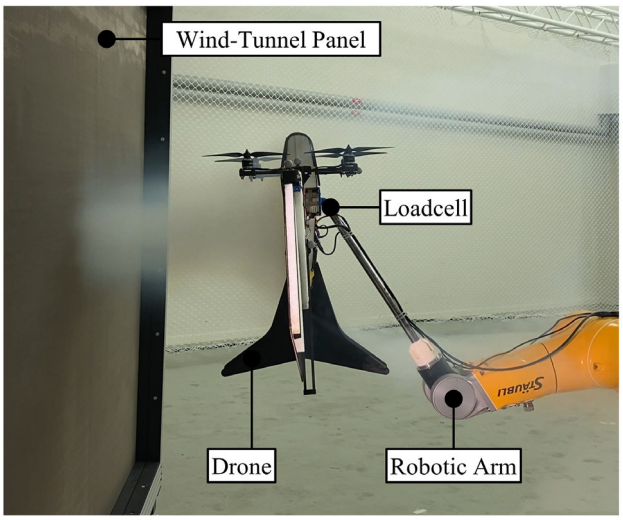

Figure 4. The aerodynamic experimental setup is composed of the drone, a Stäubli robotic arm, a WindShape wind tunnel, and an ATI Gamma F/T Sensor. The drone is at 0° angle of attack in this figure as it would be hovering.

the open wing configuration compared to the fully retracted wing configuration (Figure 5A). The aerodynamic effects in both lift and drag intensify with the increase in wind speed. Yaw moments display a significant increase in the case of asymmetric morphing configurations of one wing fully extended and one wing fully retracted at all angles, as shown in Figure 5C. The yaw moment varies from 0 Nm in the retracted wing configuration to approximately −0.8 Nm in the one wing retracted and one wing extended configuration. In comparison, the maximum yaw moment that can be generated by the motors while maintaining the drone's altitude is −0.23 Nm. This shows that the wings can significantly contribute to controlling the yaw angular rate. From Figure 5C, a linear relationship can be identified between the wing angle and the yaw moment. In addition, it is also observed that the angle of attack generally does not have a significant impact on the generated yaw moment (Figure 5E). The linearity in the wing angle–yaw moment relationship in most of the tested cases and near-constant moment suggests that an error rate P controller can be sufficient for active wing yaw stabilization.

4. Autonomous Flight Experiments

The proposed hypothesis's validation and the proposed controller's functionality require flight experiments. Each experiment was performed three times. These experiments aimed to clarify the benefits of changing symmetrically or asymmetrically the wing area while performing different flight trajectories. Flight experiments were performed in an experimental facility

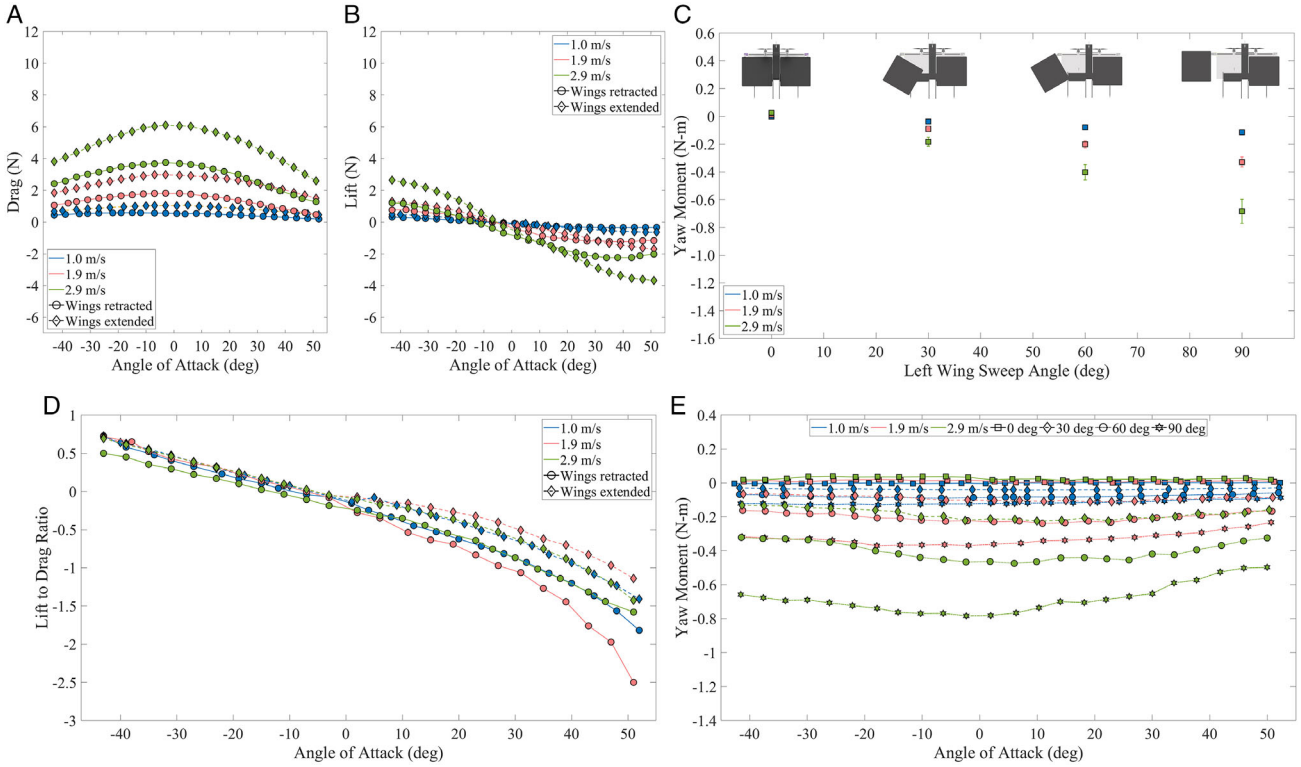

Figure 5. Aerodynamic experimental results of the different wing morphing symmetric and asymmetric configurations. A) The drag force as a function of the angle of attack at different wind speeds for the extended and retracted configurations. B) The lift force as a function of the angle of attack at different wind speeds for the extended and retracted wings configurations. C) The yaw moment generated as a function of the left wing sweep angle at different wind speeds. D) The lift to drag ratio as a function of the angle of attack at different wind speeds for the extended and retracted wings configurations. E) The yaw moment generated by the sweep of the left wing as a function of the angle of attack, at different wind speeds and sweep angles.

composed of a motion capture system of 23 cameras and a wind stream generator capable of producing different wind velocities. The generic trajectory of a drone mission in a horizontal plane can be decomposed into three main trajectories, namely, linear trajectory, rotational trajectory, and mixed trajectory composed of both previous trajectories.

As a first step toward performing a mixed trajectory, hovering at a setpoint was commanded. The wings were continuously actuated based on the yaw rate error estimated from the autopilot. The wings activation was regulated by a custom P controller. Hovering at the setpoint with a fixed orientation parallel to the wind tunnel while exposed in a wind current, the drone with active wing stabilization exceeded the performance in yaw stabilization of both fully extended and fully retracted wings. In fact the standard deviation of the yaw error decreased by 76% and 69%, respectively (Figure 7A). In addition, the position error in X remained the same, while in the Y and Z axes, it was decreased for the active wing morphing by 72% and 11% compared to the extended configuration. When compared to the retracted configuration, an increase of 14% in the position error is observed for X, while a significant improvement is displayed in Y and Z with a decrease of 48% and 26%, respectively (Figure 7A).

Continued testing of the circular trajectory (**Figure 6**D), where the plane performs a mix of linear and rotational trajectories, revealed similar results to the hovering at a setpoint experiment. The goal was to track the trajectory; the morphing wings were used for active stabilization and wind rejection. When tracking the trajectory with active wings, the standard deviation of the yaw error decreased by 58% and 49% compared to fully extended wings and fully retracted wings, respectively. Therefore, the drone with active wing morphing displayed a performance increase in yaw stabilization and the ability to better resist wind currents compared to both the extended and retracted wing configurations (**Figure 7**B). Although beneficial for increased stability and wind rejection, continuously morphing the wings might reduce the energy performance of the vehicle. Thus, in addition to the previous experiments, we investigated the impact of morphing to a fixed symmetric or asymmetric wing configuration in such a way that we use only the wings to change the drone's attitude or assist the motor's function. Linear and rotational trajectories were investigated.

At first, a linear trajectory was performed (Figure 6B). The drone was commanded to take-off, hover, and then fly, fending off the wind generator and to a given setpoint where it was commanded to land. A custom attitude controller allowed the drone to drift in the presence of wind current along the X-axis, while maintaining zero pitch (Figure 6A). The goal of the linear trajectory was to assess the operation and performance of the drone while flying with different wing configurations in the generated wind stream. The drone was placed 2.5 m from the wind generator and was commanded to a setpoint 7.5 m away inside the wind stream. In this experiment, where there is no motor contribution to the horizontal displacement, it was observed that drifting with extended wings is faster than drifting with retracted wings due to the increased drag generated by the larger area of the extended wings (**Figure 8**A). Moreover, it is able to travel faster while maintaining the same motor thrust. This means the aircraft is more controllable because it could use the motors to perform other attitude commands (Figure 8B). In addition, extended wings can reduce the drone's normalized energy consumption by 4%, 28%, and 2% for wind currents corresponding to 10%, 20%, and 30% wind power, respectively. The normalized energy consumption is calculated using the power consumption difference between the power consumed throughout the trajectory and the baseline, which is the average power required during one second in static hovering before performing the trajectory. The significant advantage is observed in middle wind current speeds. At low wind speeds, the added drag is smaller and, at high wind speeds, the drone controller tries to compensate for the generated pitching moment.

In addition to the drifting, where the motors do not actively contribute to flying throughout the commanded setpoints, experiments were performed where the drone was commanded to reach a waypoint at a speed that was set to be higher than the drifting speed with the motors contributing in extended and retracted wing configurations. The results are similar to the previous set of experiments. Extended wings always lead to lower motor saturation levels by a few percent. On the other hand, the energy depends on the wind speed. Extended wings are beneficial in the case of 20% for an 10% decrease in the normalized energy consumption. Although in the other cases, the motors consume more power to accelerate the drone when at 10% or

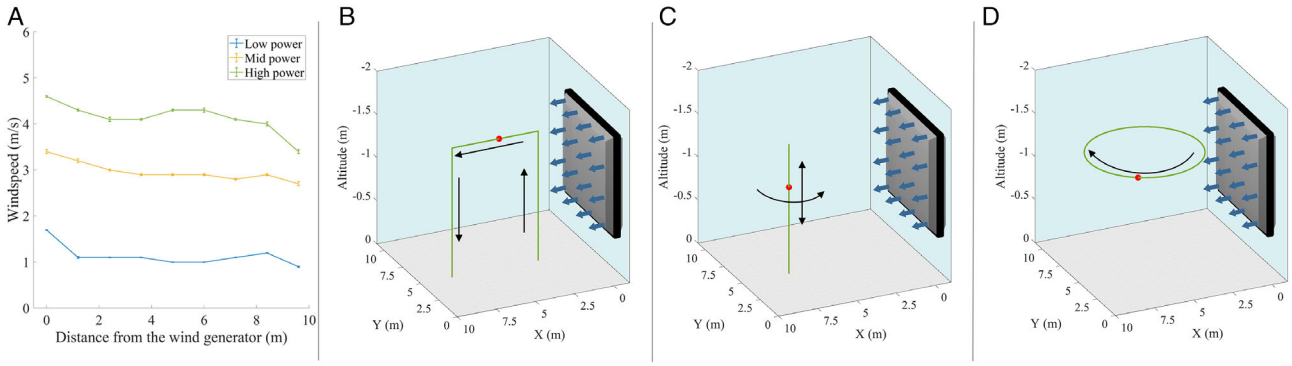

Figure 6. In this experimental setup, the wind direction is known and the state estimation of the drone is provided by a motion capture system. The wind is generated by the windshape and varies by the distance from the fan as a result of momentum loss in the flow field. A) Diagram of wind speed to distance from the wind generator. B) Linear trajectory. C) Rotational trajectory. D) Circular trajectory.

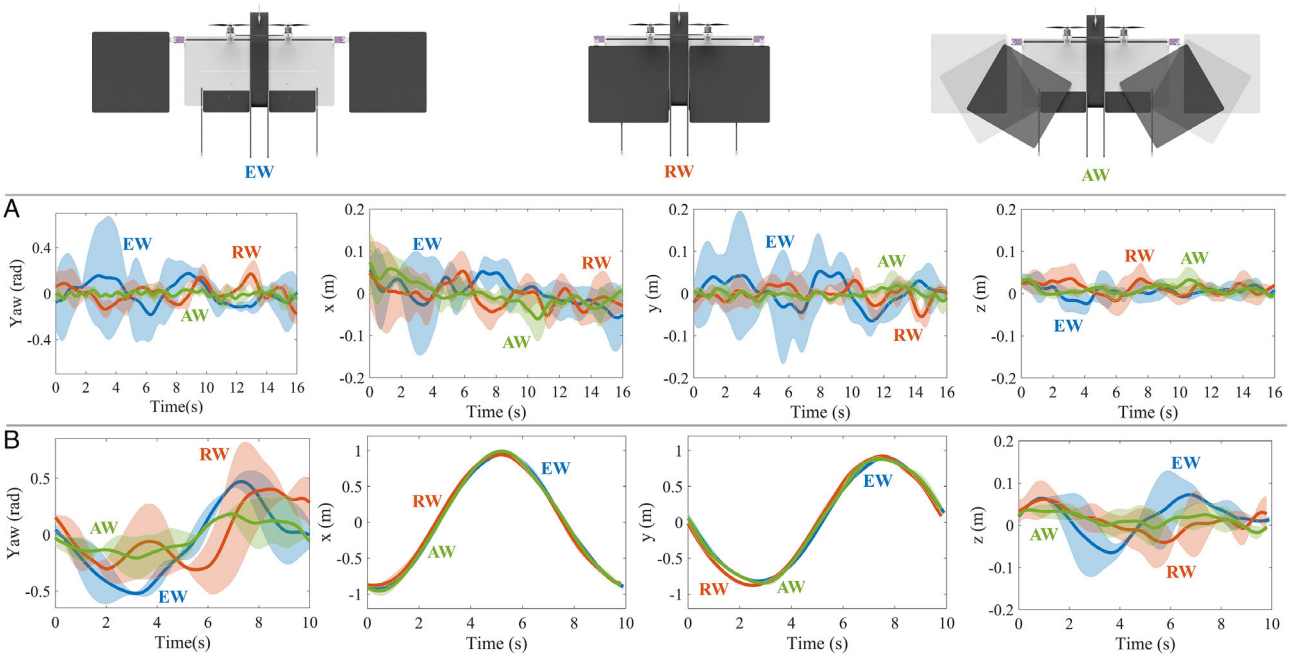

Figure 7. Flight experiments with active wing morphing for yaw stabilization and wind disturbance rejection. EW is for extended wings, RW is for retracted wings, and AW is for wings that are continuously activated. A) Hovering at a setpoint with a fixed orientation, B) hovering in circular trajectory (Figure 6D).

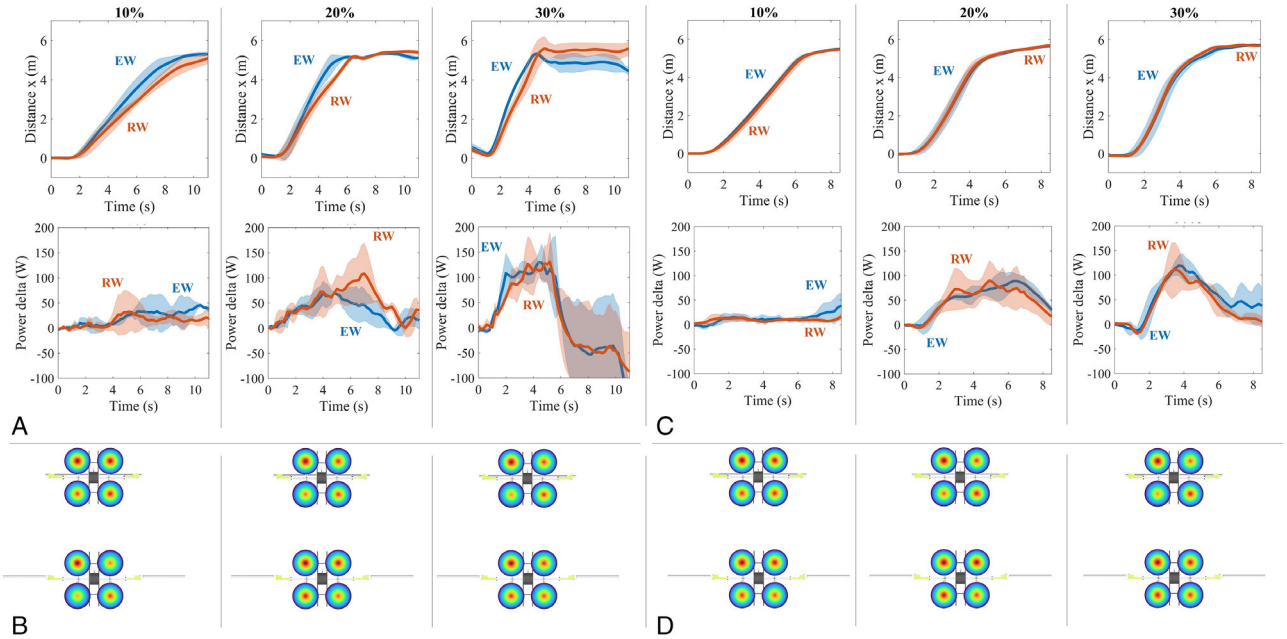

Figure 8. Drifting in linear trajectory (Figure 6B) at different wind current intensities (%) and the motor saturation levels in different wind speeds while at the extended or retracted configuration. The colored circles represent the motor pulse-width modulation (PWM) signal and thus the motor saturation. Higher change in color means higher motor saturation. EW is for extended wings, and RW is for retracted wings. A) The drone maneuvers without the motor contribution. B) Saturation levels for maneuvering without the motors contribution. C) The drone maneuvers with the motors contribution. D) Saturation levels for drone maneuvering with the motors contribution.

when they try to compensate for the adverse pitching moment generated at 30% wind power (Figure 8C,D).

The yaw authority of the drone at different wind speeds was also tested by performing rotational trajectories. This experiment aimed to determine the effect of crosswind on the performance of the drone when commanded to achieve a specific angle using pure yaw motion in hovering flight. The drone was commanded to take-off, hover, rotate to an angular setpoint, and finally land.

The drone was placed 2.5 m from the wind generator. First, a custom attitude controller allowed the drone to rotate freely while hovering at a commanded setpoint 2.5 m from the wind generator (Figure 6C). At first, the drone is tested in yaw motion with one wing fully extended, thus rotating due to only the yawing moment generated by the wing. To continue, the drone is commanded to match the rotational speed of the one wing fully extended configuration with both wings extended and both wings retracted. For the one wing extended configuration, it is observed a decrease in the energy consumption of up to 98% compared to the other configurations, as shown in **Figure 9**A. At 30% of wind current, the fully extended wings cannot perform the commanded trajectory and get destabilized by the wind current. Furthermore, the motor saturation levels for the single wing extended experiment remained lower when compared to the other configurations in most of the wind current speeds tests, thus enabling better maneuverability (Figure 9B).

In addition to the yaw experiments where the motors do not actively contribute to the yaw motion, experiments were performed where the drone was commanded to reach an angular waypoint at the highest possible speed with the motors contributing in all wing configurations. Though, the results are similar to the previous set of experiments. The experiments were conducted with extended wings, retracted wings, and one wing extended and one retracted Figure 9C. It is observed that when commanding the asymmetrical extension of one wing in synchronicity with the motors yaw command, the drone severely outperformed both the extended wing and the retracted wing configurations in terms of normalized energy efficiency by 75% and 77% for the extended wing configuration and by 20% and 51%, respectively, at wind current speed of 10% and 20%. At the same time, it is observed that at the wind current speeds of 20% and 30%, the drone reaches the angular setpoint faster and with less overshoot compared to the other wing configurations, as shown in Figure 9C. The maximum yaw rate is increased up to 200%. Motor saturation levels had a similar indication to the experiments without yaw contribution due to the impact of the asymmetric wing in the yaw maneuver, as shown in Figure 9D.

5. Discussion

The results show that continuous morphing can assist stability and wind rejection, while morphing to a fixed configuration can help exploit wind currents to increase yaw rate or increase the normalized energy efficiency significantly. Despite performing the experiments in the micro aerial vehicle scale, we expect similar behavior for larger vehicles at higher Reynolds numbers within the low Reynolds number regime of up to 150 000[1]. The same aerodynamic effects are expected to be observed because of the same behavior of flat surface in the low Reynolds number regime. Meaning that when in the deep stall, the angle of attack increases drag and decreases lift.[23] For this

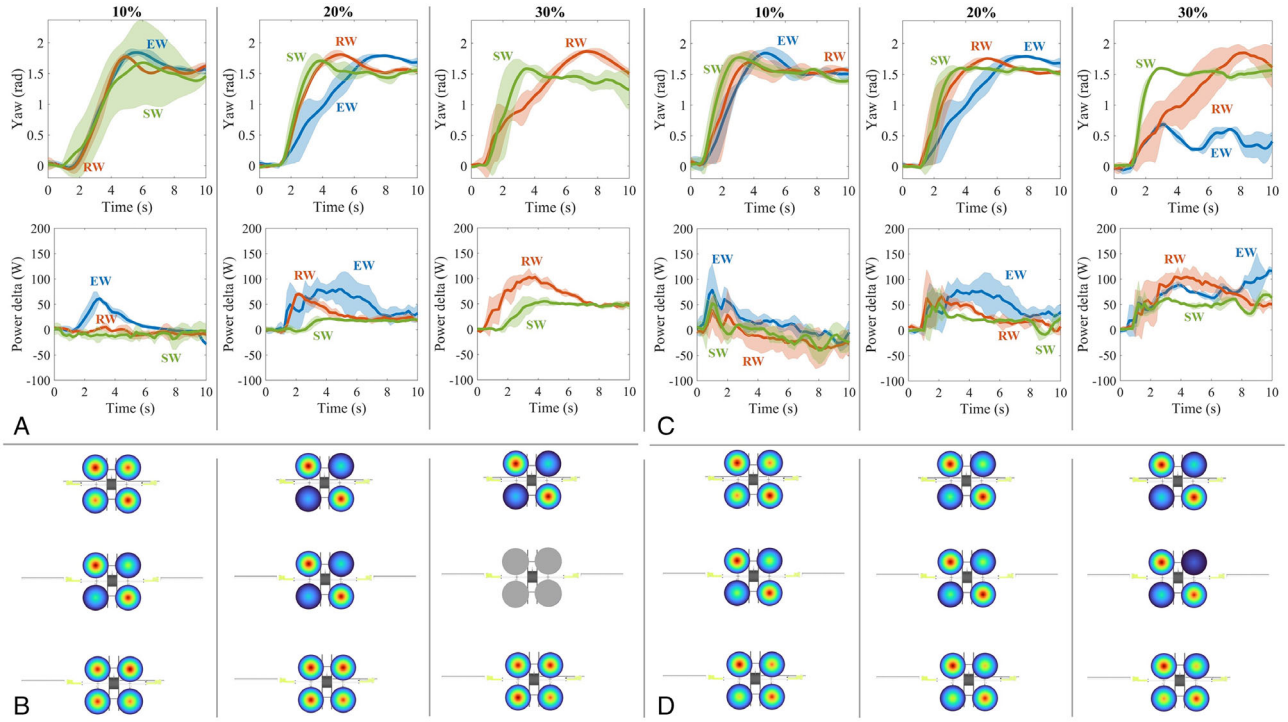

Figure 9. Yaw in rotational trajectory (Figure 6C) at different wind current intensities (%) and the motor saturation levels in different wind speeds while at the wings extended, wings retracted, or single wing extended configuration. The colored circles represent the motor PWM signal and thus the motor saturation, higher change in color means higher motor saturation. EW is for extended wings, RW is for retracted wings, and SW is for a single wing extended. A) The drone maneuvers without the motor contribution. B) Saturation levels for maneuvering without the motors contribution. C) The drone maneuvers with the motors contribution. D) Saturation levels for drone maneuvering with the motors contribution. For visualization purposes, we plot yaw from 0 to 2 rad.

study, the vehicle's shape was kept to the simplest possible as flat plates were used for the morphing wings and fuselage. Shape optimization can increase the aerodynamic benefits of continuous and noncontinuous morphing while sustaining larger wind currents. In addition to the previous discussion on the shape and structure, morphing wings also have the side benefit of increasing the agility and efficiency of the drone in horizontal flight.[11,24]

Regarding limitations, to apply the method in a real flight mission, the drone must have an accurate estimate of the wind direction and magnitude. This is because wind direction and wind force tend to change unpredictably in a natural environment. As stated before, in the experiments presented here, the wind direction is known as the drone always flies in front of the wind generator. Therefore, additional sensors or software estimators are needed for a real flight mission. At present, this type of sensors can be difficult to integrate into small vehicles. Moreover, a controller that automatically chooses between fixed or continuous wing actuation should be implemented to exploit the current method's full potential in a real flight mission. An automatic wing morphing controller would select the way of morphing depending on the mission trajectory, the effective velocity, and the wind direction changes.

6. Conclusions

This paper has shown the stability, maneuverability, and energetic benefits of a morphing wing tail-sitter UAV compared to a conventional fixed-wing configuration of the same weight. Similar results are expected to be applicable throughout the low Reynolds number regime. Additionally, the findings presented here are a promising solution for various types of drones with vertical wing surfaces, such as multimodal terrestrial and marine winged robots. Finally, the proposed method's applicability is highlighted by the fact that it can be adapted to different avionic setups or morphing wing designs as there are no specific hardware requirements. These findings indicate the potential for future aerial robotics systems not just to reject wind gusts but actively exploit them to increase range and endurance, improve agility and maneuverability, and expand the weather conditions in which UAVs can operate.

Acknowledgements

This project received funding from the European Union's Horizon 2020 research and innovation programme under the Marie Skłodowska-Curie grant agreement no. 754354. It was partially supported by NCCR Robotics, a National Centre of Competence in Research, funded by the Swiss National Science Foundation (grant number 51NF40_185543), and by the European Union's Horizon 2020 research and innovation programme under grant agreement ID: 871479 AERIAL-CORE.

Conflict of Interest

The current work has been submitted for a patent application. The authors have no conflict between them.

Data Availability Statement

The data that support the findings of this study are available from the corresponding author upon reasonable request.

Keywords

drone, morphing, UAV, VTOL, wind

Received: September 5, 2022
Revised: November 30, 2022
Published online:

[1] M. Hassanalian, A. Abdelkefi, *Progr. Aerosp. Sci.* **2017**, *91*, 99.
[2] G. J. J. Ducard, M. Allenspach, *Aerosp. Sci. Technol.* **2021**, *118*, 107035.
[3] *Modelling the Flying Bird*, Vol. *5*, 1st ed., ISSN, Elsevier Science, pp. 245, https://books.google.ch/books?id=KG86AgWwFEUC.
[4] C. Harvey, V. B. Baliga, P. Lavoie, D. L. Altshuler, *J. Roy. Soc. Interfaces* **2019**, *16*, 20180641.
[5] J. A. Cheney, J. P. J. Stevenson, N. E. Durston, J. Song, J. R. Usherwood, R. J. Bomphrey, S. P. Windsor, *Proc. Roy. Soc. B: Biol. Sci.* **2020**, *287*, 20201748.
[6] D. A. Olejnik, F. T. Muijres, M. Karásek, L. Honfi Camilo, C. De Wagter, G. C. de Croon, *Front. Robotics AI* **2022**, *9*, https://doi.org/10.3389/frobt.2022.820363.
[7] S. Mintchev, D. Floreano, *IEEE Robot. Autom. Mag.* **2016**, *23*, 42.
[8] K. Z. Y. Ang, J. Cui, T. Pang, K. Li, K. Wang, Y. Ke, B. M. Chen, in *11th IEEE Int. Conf. on Control & Automation (ICCA)*, IEEE, Piscataway, NJ **2014**, pp. 750–755.
[9] G. Heredia, A. Duran, A. Ollero, *J. Intell. Robot. Syst.* **2012**, *65*, 115.
[10] M. Di Luca, S. Mintchev, Y. Su, E. Shaw, K. Breuer, *Sci. Robot.* **2020**, *5*, eaay8533.
[11] E. Ajanic, M. Feroskhan, S. Mintchev, F. Noca, D. Floreano, *Sci. Robot.* **2020**, *5*, 47.
[12] E. Chang, L. Y. Matloff, A. K. Stowers, D. Lentink, *Science Robotics* **2020**, *5*, eaay1246.
[13] C. B. Jabeur, H. Seddik, *Int. Rev. Appl. Sci. Eng.* **2021**, *1*, 133.
[14] J. F. Whidborne, A. K. Cooke, *IFAC-PapersOnLine* **2017**, *50*, 175.
[15] Y. Yang, J. Zhu, X. Zhang, X. Wang, in *IEEE/RSJ Int. Conf. on Intelligent Robots and Systems (IROS)*, IEEE, Piscataway, NJ **2018**, pp. 6390–6396.
[16] C. Montella, J. R. Spletzer, in *IEEE/RSJ Inter. Conf. on Intelligent Robots and Systems*. IEEE, Piscataway, NJ **2014**, pp. 3423–3428.
[17] V. Bonnin, E. Benard, J.-M. Moschetta, C. A. Toomer, *Int. J. Micro Air Veh.* **2015**, *7*, 213.
[18] I. Mir, A. Maqsood, S. A. Eisa, H. Taha, S. Akhtar, *Aerosp. Sci. Technol.* **2018**, *79*, 17.
[19] Y. Zhao, A. Dutta, P. Tsiotras, M. Costello, *J. Guid. Control Dyn.* **2018**, *41*, 488.
[20] C. Vourtsis, V. Casas Rochel, F. Ramirez Serrano, W. Stewart, D. Floreano, *IEEE Rob. Autom. Lett.* **2021**, *1*, https://doi.org/10.1109/LRA.2021.3096159.
[21] C. Vourtsis, W. Stewart, D. Floreano, *IEEE Robot. Autom. Lett.* **2022**, *7*, 223.
[22] WindShape – Drone Test Equipment and Services – Wind Tunnel, https://www.windshape.ch/ (accessed: February 2021).
[23] M. Shademan, A. Naghib-Lahouti, *Adv. Aerodyn.* **2020**, *2*, 14.
[24] M. Di Luca, S. Mintchev, G. Heitz, F. Noca, D. Floreano, *Interface Focus* **2017**, 20160092.
[25] Controller Diagrams | PX4 User Guide, https://docs.px4.io/main/en/flight_stack/controller_diagrams.html (accessed: November 2022).